

BiasEnsemble: Revisiting the Importance of Amplifying Bias for Debiasing

Jungsoo Lee^{*1,2} Jeonghoon Park^{*1} Daeyoung Kim^{*1}
Juyoung Lee² Edward Choi¹ Jaegul Choo¹

¹KAIST, ²Kakao Enterprise, South Korea

¹{bebeto, jeonghoon_park, daeyoung.k, edwardchoi, jchoo}@kaist.ac.kr,

²{bebeto.lee, michael.jy}@kakaenterprise.com

Abstract

In image classification, *debiasing* aims to train a classifier to be less susceptible to dataset bias, the strong correlation between peripheral attributes of data samples and a target class. For example, even if the frog class in the dataset mainly consists of frog images with a swamp background (*i.e.*, bias-aligned samples), a debiased classifier should be able to correctly classify a frog at a beach (*i.e.*, bias-conflicting samples). Recent debiasing approaches commonly use two components for debiasing, a biased model f_B and a debiased model f_D . f_B is trained to focus on bias-aligned samples while f_D is mainly trained with bias-conflicting samples by concentrating on samples which f_B fails to learn, leading f_D to be less susceptible to the dataset bias. While the state-of-the-art debiasing techniques have aimed to better train f_D , we focus on training f_B , an overlooked component until now. Our empirical analysis reveals that removing the bias-conflicting samples from the training set for f_B is important for improving the debiasing performance of f_D . This is due to the fact that the bias-conflicting samples work as noisy samples for amplifying the bias for f_B . To this end, we propose a novel biased sample selection method *BiasEnsemble* which removes the bias-conflicting samples via leveraging additional biased models to construct a bias-amplified dataset for training f_B . Our simple yet effective approach can be directly applied to existing reweighting-based debiasing approaches, obtaining consistent performance boost and achieving the state-of-the-art performance on both synthetic and real-world datasets.

1 Introduction

When there exists a correlation between peripheral attributes and labels which is referred to as *dataset bias* [25] in the training dataset, image classification models often heavily rely on such a bias. Dataset bias is caused when the majority of data samples include bias attributes, the visual attributes that frequently co-occur with the target class but not innately defining it [18]. For example, frogs are commonly observed in swamps (bias attribute), but frogs can also be found in other places such as grasses or beaches. In such a case, the image classification model trained with the biased dataset could use swamps as the visual cue for classifying frogs. In other words, it may fail to correctly classify frog images in other places. To mitigate such an issue, debiasing aims to train the image classification model to learn the intrinsic attributes, the visual attributes which inherently define a target class, such as the legs or eyes of frogs.

In a biased dataset, the data samples without the bias attribute (*i.e.*, bias-conflicting samples) such as frogs on grasses or beaches are excessively scarce compared to the samples including the bias attributes (*i.e.*, bias-aligned samples). Due to the scarcity, existing state-of-the-art debiasing studies [18, 20] train a given model by reweighting the data samples which refers to imposing 1) high weight on losses of the bias-conflicting samples and 2) low weight on those of the bias-aligned ones. For example, Nam *et al.* reweight the data samples based on the finding that the bias attributes

* indicates equal contributions.
Preprint. Under review.

are *easy to learn* compared to the intrinsic attributes [20]. To be more specific, they intentionally train a biased model f_B to be overfitted to the easily learned bias attribute. Then, they utilize f_B for computing a reweighting value w for each training sample, which the value is designed to be high for samples f_B fails to classify (*i.e.*, bias-conflicting samples). The data items are reweighted with w during training the model f_D to learn the debiased representation. In this regard, how well f_B is overfitted to the bias attribute influences the debiasing performance since it determines the reweighting value w .

However, our careful analysis points out that f_B used in the existing reweighting-based approaches [18, 20] fail to maximally exploit the bias attribute (Section 3). They utilize a loss function which is designed to emphasize the bias-aligned samples in order to overfit f_B to bias attributes. Despite such a design, the bias-conflicting samples in a training set still work as noisy samples when training f_B to overfit to the bias since the bias-conflicting ones do not include bias attributes. Discarding the noisy samples is one straight-forward approach to handle such an issue [8, 9, 14, 23, 28, 29]. However, none of the studies shed light on removing the bias-conflicting samples from training sets for overfitting f_B to the bias attribute, especially challenging without explicit bias labels (*i.e.*, annotations of bias attributes) or prior knowledge on a certain bias.

To this end, we propose a *simple yet effective* biased sample selection method that reduces the number of bias-conflicting samples for building a refined dataset, used to amplify bias when training f_B . Using the fact that a bias attribute is learned in the *early training phase* [20], we utilize an additional biased model f_B^* pretrained for only a small number of iterations in order to 1) select samples with high confidence on the target class (*i.e.*, regarded as the bias-aligned samples) and 2) discard the ones with low confidence on the target class (*i.e.*, regarded as bias-conflicting samples). However, in the real world, one biased model may not be enough to fully learn the bias attribute since the bias attribute (*e.g.*, gender) is composed of multiple visual attributes (*e.g.*, make-up, hairstyle, beards), and there exist several different ways to learn the bias attribute. In other words, it may be challenging for a single biased model to fully exploit the various visual attributes to learn a bias attribute. Therefore, instead of utilizing a single biased model, we ensemble a multiple number of additional pretrained biased models to consider diverse visual attributes of a given bias for the purpose of refining a train dataset with bias-conflicting samples discarded. The newly refined dataset which mainly includes bias-aligned samples is then used to train f_B . Training with the bias-amplified dataset encourages f_B to maximally exploit the bias attribute when making predictions and improve the debiasing performance of f_D overall.

In summary, the main contributions of our paper are as follows:

- Based on our preliminary analysis, we reveal that how well f_B is overfitted to the bias influences the debiasing performance crucially, an important observation overlooked in the previous reweighting-based approaches.
- We propose a simple yet effective biased sample selection method termed *BiasEnsemble* which ensembles a multiple number of biased models to better capture bias attributes.
- Our method can be easily adopted in existing reweighting-based approaches, and we achieve the new state-of-the-art performances on both synthetic and real-world datasets.

2 Related Work

Existing early studies of debiasing explicitly use bias labels during training [12, 15, 24, 27] or implicitly predefine the bias types (*e.g.*, focusing on mitigating the color bias) [2, 3, 5, 6, 10, 19, 21, 26]. Bias labels or prior knowledge on the bias types are generally used to identify bias-conflicting samples. Kim *et al.* minimize the mutual information between the debiased and biased representation which requires bias labels to train biased representation [15]. Although not utilizing explicit bias labels, ReBias [3] predefines a certain bias type (*e.g.*, color and texture) and focuses on mitigating such bias by leveraging a color- and texture-oriented network with small receptive fields [4] to capture the predefined color or texture bias. However, acquiring bias labels or predefining a bias type 1) necessitates humans to identify the bias type of a given dataset and 2) limits the debiasing performance on unknown bias types [18].

Recent debiasing studies proposed several methods to address such an issue [7, 13, 18, 20]. Nam *et al.* propose LiF [20] which identifies the bias-conflicting samples based on the intuitive finding that the bias attributes are *easy to learn* compared to the intrinsic attributes. By using the fact that f_B

outputs a relatively high loss value for bias-conflicting samples, they impose high weight on (*i.e.*, emphasize) bias-conflicting samples and low weight on the bias-aligned samples during training f_D . Lee *et al.* augment the bias-conflicting samples via disentangled feature-level augmentation, emphasizing them along with the bias-conflicting samples in the original training set by using the reweighting method [18]. Although the previous studies utilize f_B for computing the reweighting value, we reveal that they overlooked the importance of amplifying bias for f_B which is crucial for improving the debiasing performance of f_D .

3 Importance of Amplifying Bias

This section elaborates on the importance of amplifying bias in f_B for improving the debiasing performance of f_D . We first describe how the existing state-of-the-art debiasing approaches utilize f_B to reweight the data samples (Section 3.1). Then, we show that amplifying bias in training f_B is crucial for improving debiasing performance of f_D which was overlooked in the previous studies (Section 3.2).

3.1 Background

Overfitting model to the bias Since annotating bias labels or identifying the bias types in advance is challenging and labor intensive [18], recent studies leverage the Generalized Cross Entropy (GCE) loss [30] that does not require such information for amplifying the bias [18, 20]. The GCE loss is defined as:

$$\mathcal{L}_{\text{GCE}}(p(x; \theta), y) = \frac{1 - p_y(x; \theta)^q}{q}, \quad (1)$$

where q is a hyper-parameter that regulates the degree of amplification, and $p(x; \theta)$ and $p_y(x; \theta)$ are the softmax output of the network parameterized by θ and the softmax probability of the target class y , respectively. The GCE loss assigns high weights on the gradients of the samples with the high prediction probability on the target class y , which can be formulated as:

$$\frac{\partial \mathcal{L}_{\text{GCE}}(p, y)}{\partial \theta} = p_y^q \frac{\partial \mathcal{L}_{\text{CE}}(p, y)}{\partial \theta}. \quad (2)$$

When trained with a biased dataset, GCE loss encourages the model to focus on the easy samples with high probability values. As revealed in the work of Nam *et al.*, the bias attributes are easy to learn compared to the intrinsic attributes, so a model predicts bias-aligned samples with high probability values [20]. Due to this fact, the GCE loss encourages the model to focus mainly on the bias-aligned samples, leading the model to be biased overall.

Reweighting-based approaches Recent state-of-the-art debiasing methods [18, 20] reweight data samples by utilizing two different models: 1) a biased model f_B and 2) a debiased model f_D . The former one is trained to be overfitted to the bias attribute while the latter one is mainly trained with the bias-conflicting samples, those which are identified by utilizing f_B . To be more specific, since f_B heavily relies on the bias attributes for making predictions, it fails to correctly classify the bias-conflicting samples, those without the bias attributes. Due to this fact, the Cross Entropy (CE) loss values of bias-conflicting samples are relatively high compared to those of bias-aligned ones. By utilizing such a characteristic, the loss of each data sample x is reweighted for training f_D with the reweighting value $w(x)$. Specifically, Nam *et al.* [20] formulated $w(x)$ as

$$w(x) = \frac{\mathcal{L}_{\text{CE}}(f_B(x), y)}{\mathcal{L}_{\text{CE}}(f_B(x), y) + \mathcal{L}_{\text{CE}}(f_D(x), y)}, \quad (3)$$

where $f_B(x)$ and $f_D(x)$ indicate the prediction outputs of f_B and f_D , respectively, and y is the target label of the sample x . Using the formula, the reweighting value $w(x)$ is designed to be imposed 1) high for the bias-conflicting samples and 2) low for the bias-aligned samples in order to improve the debiasing performance of f_D . In this regard, how well f_B is overfitted to the bias attribute determines the $w(x)$ which crucially influences the debiasing performance of f_D .

3.2 Revisiting f_B in Reweighting-based Debiasing Methods

In this section, we show that the existing state-of-the-art reweighting methods fail to fully overfit f_B to the bias, resulting in an unsatisfactory reweighting of the data samples during training f_D overall. For the experiments, we use Colored MNIST [18] and biased FFHQ (BFFHQ) [16] to demonstrate

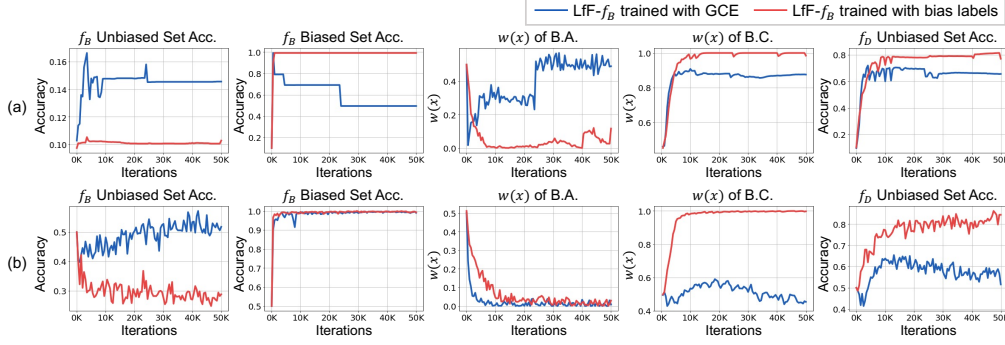


Figure 1: Comparison of LfF utilizing f_B trained with 1) GCE loss (blue) and 2) explicit bias labels (red). (a) and (b) indicate the results on Colored MNIST and BFFHQ, respectively. Starting from the first column, each graph represents the 1) unbiased test set accuracy of f_B , 2) biased test set accuracy of f_B , 3) averaged reweighting value $w(x)$ of bias-aligned samples (abbreviated as B.A.), 4) that of bias-conflicting samples (abbreviated as B.C.), and 5) unbiased test set accuracy of f_D .

that our analysis is applicable both on synthetic and real-world datasets. Bias-conflicting samples consist 1% of both training sets in this analysis. Detailed descriptions of the datasets are included in Section 5.1 and Supplementary. In Fig. 1, we compare 1) LfF [20] training f_B with GCE loss (blue) and 2) LfF training f_B with explicit bias labels using Cross Entropy (CE) loss (red). For the evaluation, we use 1) a biased test set, a dataset having a similar data distribution as the biased training set, and 2) the unbiased test set, a dataset which has no correlation found in the biased training set.

Imperfectly biased f_B A fully biased f_B is likely to achieve 1) high accuracy on the biased test set and 2) low accuracy on the unbiased test set since it only uses the bias attribute as the visual cue for predictions. In other words, the gap between the biased test set accuracy and the unbiased test set accuracy increases as f_B focuses on the bias attribute. As shown in Fig. 1, however, f_B trained with GCE loss (blue) shows relatively higher unbiased test set accuracy compared to f_B trained with the explicit bias labels (red). Assuming that f_B trained with the explicit bias labels is perfectly overfitted to the bias attribute, such results demonstrate that f_B trained with GCE loss is less overfitted to the bias. The main reason for such a result is that the bias-conflicting samples in the training set work as noisy samples when overfitting f_B to the bias. Although GCE loss mitigates such an issue by imposing high gradients on the bias-aligned samples, we observe that the noisy samples (*i.e.*, bias-conflicting samples) still prevent f_B from being fully overfitted to the bias.

Debiasing f_D via f_B The reweighting value $w(x)$ determines the degree of how much f_D should focus on a given sample x during the training phase. It is crucial to satisfy two conditions simultaneously for training a debiased classifier f_D : imposing 1) high $w(x)$ on the bias-conflicting samples and 2) low $w(x)$ on the bias-aligned samples. In other words, the difference between $w(x)$ of bias-conflicting samples and that of bias-aligned samples, $w(x)_{\text{diff}}$, should be large in order to improve the debiasing performance. We observe that LfF trained with GCE loss, however, outputs relatively small $w(x)_{\text{diff}}$ compared to LfF trained with explicit bias labels (third and fourth column in Fig. 1). The main reason is due to utilizing a less overfitted f_B for computing $w(x)$. Low $w(x)$ on bias-conflicting samples indicates that they are less emphasized in training f_D , which should be emphasized for learning debiased features (fourth column in Fig. 1). Therefore, f_D of LfF trained with GCE loss shows lower test accuracy than the one trained with explicit bias labels (fifth column in Fig. 1). Based on the finding that how well f_B is overfitted to the bias significantly influences the debiasing performance of f_D , we propose an approach which further amplifies the bias for training f_B .

4 Debiasing via BiasEnsemble

Inspired by the experiments in Section 3, we propose a novel biased sample selection method BiasEnsemble (BE) which filters out the bias-conflicting samples to encourage f_B to maximally exploit the bias attribute. BE (Fig. 2 (a)) works in the following procedure: 1) we build a bias-conflicting detector (BCD) and 2) construct a bias-amplified dataset \mathcal{D}_A by filtering out the bias-conflicting samples from the original training set \mathcal{D} via ensembling multiple BCDs. After that, we train f_B with \mathcal{D}_A while training f_D with the original training set \mathcal{D} by using the existing reweighting-based debiasing methods [18, 20] (Fig. 2 (b)). The details of each process are explained in the following sections.

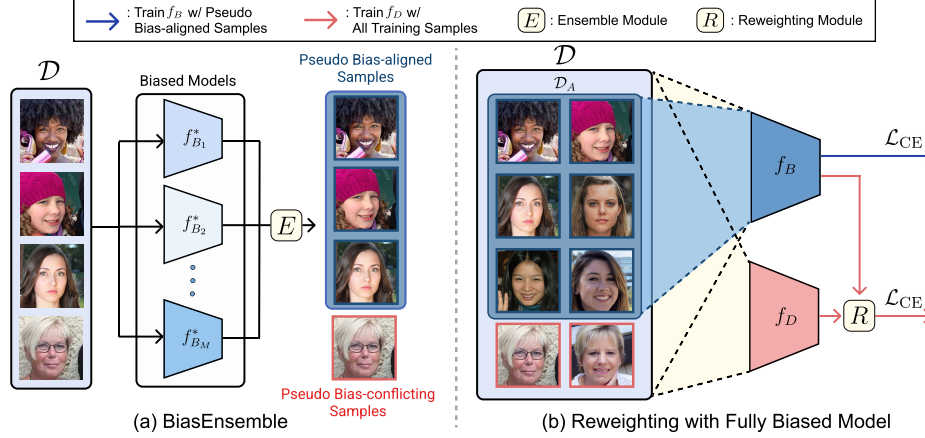


Figure 2: Illustration of our proposed method. (a) By filtering out pseudo bias-conflicting samples detected via ensembling M pretrained biased models ($f_{B_1}^*, \dots, f_{B_M}^*$), we obtain the bias-amplified dataset \mathcal{D}_A . (b) Then, we train f_B with \mathcal{D}_A while training f_D with the original training set \mathcal{D} . E and R indicate the ensemble and reweighting modules, respectively. Although not used for training f_B , the pseudo bias-conflicting samples are still fed to f_B for obtaining the reweighting value used for training f_D .

4.1 Detecting Bias-conflicting Samples

Our main goal is to obtain a bias-amplified dataset which does not contain the bias-conflicting samples in order to enforce f_B to make predictions based only on the bias attribute. We pretrain an additional biased model f_B^* with GCE loss for a *small number of iterations* by utilizing the property that the bias attribute is easy to learn in the early training phase [20]. Note that f_B^* is a pretrained biased model while f_B is the biased model used for reweighting data samples during training f_D .

Since f_B^* is overfitted to the bias at a certain degree, it mainly 1) correctly classifies the bias-aligned samples and 2) misclassifies the bias-conflicting samples. In other words, the model outputs high confidence (*i.e.*, the softmax probability) on the target class for the bias-aligned samples while low confidence for the bias-conflicting samples. By utilizing the probability of the target class p_y , we build the bias-conflicting detector BCD as follows:

$$BCD(x; \tau, f) = \begin{cases} 0, & \text{if } p_y(x; f) < \tau \\ 1, & \text{if } p_y(x; f) \geq \tau \end{cases}, \quad (4)$$

where τ is the confidence threshold. The detector regards the samples with confidence higher than the threshold as bias-aligned samples and vice versa.

4.2 BiasEnsemble

While a single BCD may discard the bias-conflicting samples at a reasonable level, we empirically found that constructing \mathcal{D}_A relying on only a single BCD shows large performance variations (Table 3 and Table 4). Although the bias attribute (*e.g.*, gender bias) is easy to learn compared to the intrinsic attribute in the early training phase, it may form as a combination of multiple visual attributes (*e.g.*, make-up, hairstyle, beards), especially in the real-world datasets. Due to this fact, differently initialized models may focus on different visual attributes for learning the bias attribute. For example, one BCD might capture the gender bias of a female image by mainly using the long hair as the visual cue while the other may recognize the bias mainly due to the heavy make-up. Thus, each BCD may make different predictions on a same sample, leading to performance variation overall. One of the straight-forward solutions is considering both visual attributes to predict gender bias (*i.e.*, predicting an image as female if it includes both heavy make-up and long hair). In other words, leveraging a multiple number of BCDs enables considering diverse visual attributes of a given bias attribute, better capturing the bias than using a single BCD. Note that we provide GradCAM [22] visualizations which show that each model captures different visual attributes for learning a bias attribute in our Supplementary.

To this end, we propose BE which selects data samples based on the predictions of multiple BCDs. To be more specific, we leverage multiple pretrained biased models ($f_{B_1}^*, f_{B_2}^*, \dots, f_{B_M}^*$). All models



Figure 3: Illustrative examples of datasets utilized in this work. Each column in four datasets corresponds to each class. The images above the dotted line are the bias-aligned samples, while the ones below indicate the bias-conflicting samples. Detailed descriptions and additional examples of the datasets are included in Supplementary.

have the same architecture as f_B , but each model is differently initialized. Note that we utilize the property that bias attribute is learned in the *early training phase* [20], so we only need a negligible training time for each f_B^* . Then, M number of BCDs are built using each pretrained biased model f_B^* following Section 4.1. Finally, we discard the sample that the majority of the detectors consider as the bias-conflicting sample (*i.e.*, majority voting). For example, setting $M = 5$, a given sample is regarded as the bias-conflicting sample if more or equal to three BCDs voted it as the bias-conflicting one. In summary, BE can be formulated as

$$BE(x; \tau, \{f_{B_1}^*, \dots, f_{B_M}^*\}) = \begin{cases} 0, & \text{if } \sum_{i=1}^M BCD(x; \tau, f_{B_i}^*) < \lceil \frac{M}{2} \rceil, \\ 1, & \text{if } \sum_{i=1}^M BCD(x; \tau, f_{B_i}^*) \geq \lceil \frac{M}{2} \rceil, \end{cases} \quad (5)$$

where M is the number of BCDs used in BE. Finally, the data samples selected from BE are labeled as pseudo bias-aligned samples which consist of \mathcal{D}_A , used for training f_B .

4.3 Training Debaised Model Using BE

After obtaining a bias-amplified dataset \mathcal{D}_A which contains a significantly smaller number of bias-conflicting samples compared to the original training dataset \mathcal{D} , we train f_B using \mathcal{D}_A . When applying BE to existing reweighting-based approaches, LfF [20] and DisEnt [18], we do not modify the training procedure of f_D . Thus, BE can be easily applied to existing methods that leverage f_B for reweighting data samples. Note that f_B is utilized for reweighting all the training data samples during training f_D , although the pseudo bias-conflicting ones (*i.e.*, the samples not included in \mathcal{D}_A) are not used for training f_B . Both f_B and f_D are trained with the CE loss.

5 Experiment

This section describes the experimental settings (Section 5.1), demonstrates the effectiveness of BE via extensive quantitative evaluations (Section 5.2), and presents in-depth analyses (Section 5.3). For all experiment results, best performing results are shown in bold. Note that we include additional in-depth analyses in Supplementary that we could not present due to page limit.

5.1 Experimental Settings

Dataset Following the previous studies, we conduct experiments under four datasets: Colored MNIST [18], biased FFHQ (BFFHQ) [16], Dogs & Cats [15], and biased action recognition (BAR) [20]. As shown in Fig. 3, each dataset has an intrinsic attribute and a bias attribute: Colored MNIST - {digit, color}, BFFHQ - {age, gender}, Dogs & Cats - {animal, color}, and BAR - {action, background}. The former and latter visual attribute in the bracket correspond to the intrinsic and bias attribute, respectively. We conduct experiments under various ratios of bias-conflicting samples (*i.e.*, the number of bias-conflicting samples out of the total number of training samples) in each dataset to evaluate the debiasing algorithms under different levels of bias severity, following the previous studies [18, 20]. For evaluating the debiasing performance, we use unbiased test sets which include images without the correlation found in the training set. We use datasets with 1% ratio of bias-conflicting samples when conducting the in-depth analyses.

Baselines We compare our method against seven baselines of debiasing methods: Vanilla, Hex [26], LNL [15], EnD [24], ReBias [3], LfF [20], and DisEnt [18]. We denoted whether each debiasing method 1) requires explicit bias labels and 2) predefines a bias type by using check marks and cross

Table 1: Image classification accuracies on unbiased test sets with varying ratios of bias-conflicting samples. We intentionally omit the standard deviation due to the page limit which we include in the Supplementary. The *cross* and *check* represent whether each model 1) uses bias labels during training and 2) requires predefined bias type. For applying BE on LfF and DisEnt, the performance gains are shaded in grey. Best performing results are marked in bold.

Dataset	Ratio (%)	Vanilla [11]	HEX [26]	LNL [15]	EnD [24]	ReBias [3]	LfF [20]	DisEnt [18]	LfF+BE		DisEnt+BE	
		<i>xx</i>	<i>x✓</i>	<i>✓✓</i>	<i>✓✓</i>	<i>x✓</i>	<i>xx</i>	<i>xx</i>	<i>xx</i>		<i>xx</i>	
Colored MNIST	0.5	34.75	42.25	36.29	35.33	60.86	63.55	68.49	69.70	(+ 6.15)	71.34	(+ 2.85)
	1.0	51.14	47.02	49.48	48.97	82.78	76.81	79.99	81.17	(+ 4.36)	82.11	(+ 2.12)
	2.0	65.72	72.82	63.30	67.01	92.00	84.18	84.09	85.20	(+ 1.02)	84.66	(+ 0.57)
	5.0	82.82	85.50	81.30	82.09	96.45	89.65	89.91	90.04	(+ 0.39)	90.15	(+ 0.24)
BFFHQ	0.5	55.64	56.96	56.88	55.96	55.76	65.19	62.08	67.36	(+ 2.17)	67.56	(+ 5.48)
	1.0	60.96	62.32	62.64	60.88	60.68	69.24	66.00	75.08	(+ 5.84)	73.48	(+ 7.48)
	2.0	69.00	70.72	69.80	69.72	69.60	73.08	69.92	80.32	(+ 7.24)	79.48	(+ 9.56)
	5.0	82.88	83.40	83.08	82.88	82.64	79.80	80.68	85.48	(+ 5.68)	84.84	(+ 4.16)
Dogs & Cats	1.0	48.06	46.76	50.90	48.56	48.70	71.72	65.74	81.52	(+ 9.80)	80.74	(+ 15.00)
	5.0	69.88	72.60	73.96	68.24	65.74	84.32	81.58	88.60	(+ 4.28)	86.84	(+ 5.26)
BAR	1.0	70.55	70.48	70.65	71.07	73.04	70.16	70.33	73.36	(+ 3.20)	73.29	(+ 2.96)
	5.0	82.53	81.20	82.43	82.78	83.90	82.95	83.13	83.87	(+ 0.92)	84.96	(+ 1.83)

marks. We apply BE to the state-of-the-art reweighting-based debiasing methods: 1) LfF and 2) DisEnt.

Implementation details Following Nam *et al.* [20] and Lee *et al.* [18], we use a multi-layer perceptron (MLP) which consists of three hidden layers for Colored MNIST. For the other datasets except for BAR, we train ResNet18 [11] from the random initialization. Since BAR has an extremely small number of images compared to other datasets, we utilize a pretrained ResNet18. We set $M=5$ in BE, meaning that we pretrain five biased models (*i.e.*, $f_{B_1}^*, f_{B_2}^*, \dots, f_{B_5}^*$). While all experiments are trained for 50K iterations, each f_B^* is pretrained for 1K iterations on all datasets, requiring negligible amount of additional computational costs. We set the confidence threshold τ for the BCD as 0.99. Note that all the hyper-parameters are constant across all datasets and bias severities. We report the mean of the best unbiased test set accuracy over five independent trials. We include the remaining details of datasets, baselines, and implementation in the Supplementary.

5.2 Comparisons on Unbiased Test Sets

Table 1 compares the image classification accuracies of the debiasing approaches on the unbiased test sets. As aforementioned, we applied BE on the state-of-the-art reweighting-based approaches, LfF [20] and DisEnt [18]. We found that using BE for the two methods significantly improves the debiasing performances in four datasets regardless of the bias severities. The performance gains are colored grey in the background in Table 1. We also observe that using BE brings larger performance gain when evaluated with real-world datasets compared to the synthetic dataset. For example, adding BE on DisEnt shows 7.48% and 9.56% performance gain on BFFHQ with 1% and 2% ratio of bias-conflicting samples, respectively.

Adding BE on DisEnt outperforms ReBias [3] on BAR. BAR dataset is biased towards the background which mainly contains the color and texture bias. Since ReBias uses BagNet [4] which is a color- and texture-oriented model to identify bias (*i.e.*, leveraging a prior knowledge on the bias type), it showed the state-of-the-art performance before adding BE on existing reweighting-based approaches. However, even without such prior knowledge on the bias type, adding BE on DisEnt outperforms ReBias regardless of bias severities.

For the Colored MNIST, ReBias utilizes four layers of convolutional neural network while the other debiasing methods use three layers of multi-layer perceptron. We inevitably use the convolutional neural network for ReBias since it leverages a small receptive field of convolutional layers to capture the color bias. When comparing with the baselines using the same architecture, adding BE on LfF and DisEnt achieves the state-of-the-art debiasing performance on Colored MNIST.

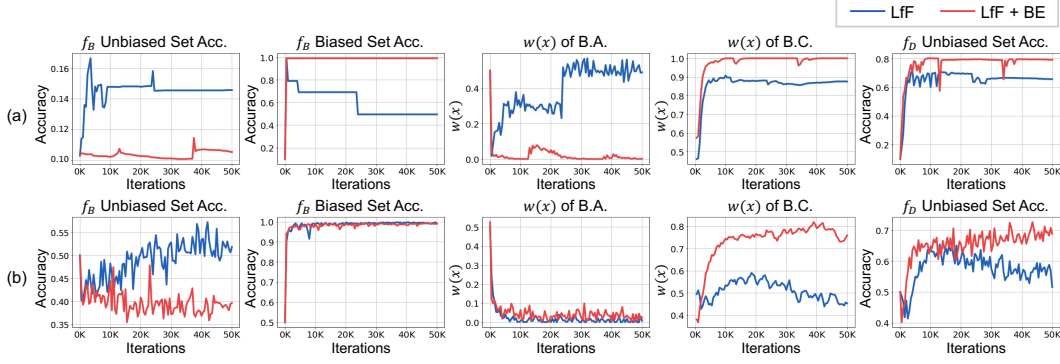


Figure 4: Comparison of LfF trained 1) without BE (blue) and 2) with BE (red) on (a) Colored MNIST and (b) BFFHQ. Each column corresponds to the ones in Fig. 1.

5.3 Analysis

Amplified bias of f_B via BE Similar to Fig. 1 which describes the motivation of our work, we compare LfF trained 1) without BE and 2) with BE in Fig. 4. While achieving comparable or higher biased test set accuracy, f_B with BE shows lower unbiased test set accuracy compared to f_B without BE. This leads to increase the $w(x)_{\text{diff}}$, the difference between $w(x)$ of bias-conflicting samples and that of bias-aligned ones. Then, bias-conflicting samples are further emphasized for training f_D , improving the debiasing performance overall. Such improvement is valid in both synthetic dataset (*i.e.*, Colored MNIST) and the real-world dataset (*i.e.*, BFFHQ). This visualization demonstrates that our proposed method indeed improves debiasing performance of f_D by further amplifying bias of f_B .

How to construct bias-amplified \mathcal{D}_A for debiasing We found two important factors when constructing \mathcal{D}_A : 1) discarding sufficient number of bias-conflicting samples and 2) maintaining a reasonable number of bias-aligned ones. To understand how the data samples composing \mathcal{D}_A affects the debiasing performance, Table 2 compares the debiasing performances of LfF by adjusting the number of bias-aligned and bias-conflicting samples in \mathcal{D}_A . In Table 2, # of B.A. and # of B.C. indicate the remaining number of bias-aligned samples and that of bias-conflicting samples in \mathcal{D}_A , respectively, computed in ratio compared to the original training set. For example, in the case of adjusted ratios of (20%, 20%), 50000 bias-aligned samples and 100 bias-conflicting samples in \mathcal{D} are adjusted to 10000 and 20 in \mathcal{D}_A , respectively. We trained f_B by using the adjusted dataset while using the original training dataset for training f_D .

When fixing the number of bias-aligned samples constant (100%), the debiasing performance increases as the number of bias-conflicting samples decreases (from 80% to 20%). The main reason is that the bias-conflicting samples, those working as noisy samples for f_B to learn the bias attribute, are discarded. This demonstrates that discarding sufficient number of bias-conflicting samples is important for improving debiasing performance which is straight-forward. On the other hand, we also observe that debiasing performance also deteriorates when the number of bias-aligned samples decreases (from 80% to 20%) with the constant number of bias-conflicting samples (20%). This indicates that f_B also requires a sufficient number of bias-aligned samples to learn the bias attributes. We want to emphasize that simply discarding numerous number of training samples for the purpose of eliminating entire bias-conflicting samples can rather aggravate the debiasing performance since it also filters out bias-aligned ones, those important for learning a bias. This analysis demonstrates the importance of considering both factors when constructing \mathcal{D}_A .

Table 2: Unbiased test set accuracies with adjusted number of bias-aligned samples (# of B.A.) and that of bias-conflicting ones (# of B.C.) in the bias-amplified dataset \mathcal{D}_A utilized for training f_B of LfF. The values in the first two rows represent the ratio of samples in \mathcal{D}_A compared to \mathcal{D} .

	# of B.A.	100%	100%	100%	100%	100%	20%	40%	60%	80%
	# of B.C.	100%	80%	60%	40%	20%	20%	20%	20%	20%
Colored MNIST	58.48 \pm 2.78	66.47 \pm 2.86	73.87 \pm 2.55	77.87 \pm 3.30	81.58 \pm 0.68	63.21 \pm 2.86	73.86 \pm 2.31	75.75 \pm 5.10	79.82 \pm 0.65	
BFFHQ	62.10 \pm 0.79	69.88 \pm 0.83	73.96 \pm 2.44	77.60 \pm 1.72	79.36 \pm 1.43	69.12 \pm 1.12	72.20 \pm 0.88	75.88 \pm 2.57	78.52 \pm 1.19	
Dogs&Cats	53.10 \pm 4.80	61.18 \pm 3.70	71.00 \pm 2.85	75.38 \pm 3.27	79.22 \pm 2.83	60.78 \pm 3.53	60.58 \pm 2.18	63.86 \pm 4.49	71.80 \pm 2.04	

Table 3: Unbiased test set accuracies on 1) LfF, 2) applying BE on LfF with a single BCD and 3) multiple BCDs. M indicates the number of BCDs when using BE.

Method	M	Colored MNIST	BFFHQ	Dogs & Cats	BAR
LfF	-	76.81 \pm 4.56	69.24 \pm 2.07	71.72 \pm 4.56	70.16 \pm 0.77
LfF + BE	1	79.51 \pm 1.56	71.52 \pm 2.68	76.98 \pm 6.63	71.63 \pm 1.59
	5	81.17 \pm 0.68	75.08 \pm 2.29	81.52 \pm 1.13	73.36 \pm 0.97

Table 4: The remaining number of bias-aligned samples (# of B.A.) and bias-conflicting ones (# of B.C.) in the bias-amplified dataset \mathcal{D}_A after applying BE. The remaining numbers are shown in ratios of samples compared to the original training dataset \mathcal{D} .

M	Colored MNIST		BFFHQ		Dogs & Cats		BAR	
	# of B.A.(%) \uparrow	# of B.C.(%) \downarrow	# of B.A.(%) \uparrow	# of B.C.(%) \downarrow	# of B.A.(%) \uparrow	# of B.C.(%) \downarrow	# of B.A.(%) \uparrow	# of B.C.(%) \downarrow
1	84.10 \pm 11.01	4.64 \pm 0.79	84.51 \pm 4.34	24.47 \pm 4.63	85.89 \pm 2.61	12.00 \pm 6.25	97.24 \pm 0.27	60.00 \pm 13.24
5	99.96 \pm 0.03	1.42 \pm 0.78	92.22 \pm 0.26	24.37 \pm 3.07	88.60 \pm 1.02	9.50 \pm 3.75	98.39 \pm 0.19	51.42 \pm 5.34

Superiority of multiple BCDs over single BCD We compare the debiasing performance of using BE with a single BCD ($M = 1$) and multiple BCDs ($M = 5$) on LfF in Table 3. While using a single BCD brings performance gain compared to LfF, the standard deviation of the performance is larger when compared to using multiple BCDs. For example, using a single BCD to train LfF shows the standard deviation of 6.63% on Dogs & Cats dataset. This is due to the fact that we rely on a single BCD for constructing \mathcal{D}_A . When the single BCD fails to be overfitted to the bias, it fails to filter out the bias-conflicting samples for building \mathcal{D}_A . However, such an issue is mitigated when using multiple BCDs since they better capture the bias attribute by considering multiple visual attributes of the bias, compared to using a single BCD. We provide the further analysis on the performance variations of single BCD and multiple BCDs in Supplementary.

Such result is mainly due to the number of bias-aligned samples and bias-conflicting ones included in \mathcal{D}_A , as demonstrated in Table 2. Table 4 shows the remaining number of bias-aligned samples and bias-conflicting samples in \mathcal{D}_A after applying BE, each computed in ratio compared to the original training dataset \mathcal{D} . We observe that utilizing multiple BCDs in BE 1) significantly increases the number of aligned samples and 2) further reduces the number of bias-conflicting samples compared to using a single BCD. Additionally, the standard deviations of the remaining number of samples are considerably larger when using the single BCD, demonstrating that a single BCD fails to fully capture the bias attribute at a stable level.

Table 5: Unbiased test set accuracies evaluated with a wide range of confidence threshold τ of BE.

Method	LfF	LfF + BE				
Threshold	-	0.9	0.95	0.98	0.99	0.999
Colored MNIST	76.81 \pm 4.56	80.65 \pm 1.88	80.49 \pm 2.16	80.41 \pm 1.51	81.17 \pm 0.68	81.06 \pm 0.86
BFFHQ	69.24 \pm 2.07	73.16 \pm 1.90	74.48 \pm 0.89	74.28 \pm 1.78	75.08 \pm 2.29	72.32 \pm 1.57
Dogs & Cats	71.72 \pm 4.56	80.60 \pm 2.87	77.66 \pm 3.37	80.36 \pm 2.69	81.52 \pm 1.13	77.90 \pm 1.50
BAR	70.16 \pm 0.77	71.53 \pm 1.98	72.23 \pm 0.45	73.00 \pm 1.52	73.36 \pm 0.97	71.28 \pm 0.88

Robustness of BE across τ . Table 5 shows that BE is robust to the confidence threshold τ . We report the image classification accuracy on the unbiased test set using a wide range of τ (*i.e.*, from 0.9 to 0.999). We observe that the test set accuracies constantly improve by applying BE compared to LfF, regardless of the value of τ .

6 Conclusion

In this work, we propose a biased sample selection method named *BiasEnsemble* in order to train f_B to maximally exploit the bias attribute when making predictions. Our main finding is that how well f_B is overfitted to the bias influences the debiasing performance of f_D which was overlooked in the previous debiasing studies. While training f_B to overfit to the bias, the bias-conflicting samples work as noisy samples, so we filter them out to construct a refined bias-amplified dataset \mathcal{D}_A . To do so, we ensemble additional pretrained biased models with the negligible number of additional iterations and use the data samples which the majority of the models regarded as bias-aligned samples for constructing \mathcal{D}_A . Despite its simple approach, BE improves recent state-of-the-art reweighting-based debiasing approaches over four different datasets with various bias severities. We believe that we shed light on an important debiasing component f_B which has been overlooked, and future researchers utilize the lessons and findings from our work to further improve the debiasing performance.

References

- [1] Dogs vs. cats redux: Kernels edition.
- [2] Aishwarya Agrawal, Dhruv Batra, and Devi Parikh. Analyzing the behavior of visual question answering models. In *Proceedings of the 2016 Conference on Empirical Methods in Natural Language Processing*, pages 1955–1960, Austin, Texas, November 2016. Association for Computational Linguistics.
- [3] Hyojin Bahng, Sanghyuk Chun, Sangdoo Yun, Jaegul Choo, and Seong Joon Oh. Learning de-biased representations with biased representations. In *International Conference on Machine Learning (ICML)*, 2020.
- [4] Wieland Brendel and Matthias Bethge. Approximating cnns with bag-of-local-features models works surprisingly well on imagenet. *International Conference on Learning Representations*, 2019.
- [5] Remi Cadene, Corentin Dancette, Hedi Ben younes, Matthieu Cord, and Devi Parikh. Rubi: Reducing unimodal biases for visual question answering. In H. Wallach, H. Larochelle, A. Beygelzimer, F. d’Alché-Buc, E. Fox, and R. Garnett, editors, *Advances in Neural Information Processing Systems*, volume 32. Curran Associates, Inc., 2019.
- [6] Christopher Clark, Mark Yatskar, and Luke Zettlemoyer. Don’t take the easy way out: Ensemble based methods for avoiding known dataset biases. In *Proceedings of the 2019 Conference on Empirical Methods in Natural Language Processing and the 9th International Joint Conference on Natural Language Processing (EMNLP-IJCNLP)*, pages 4069–4082, Hong Kong, China, November 2019. Association for Computational Linguistics.
- [7] Luke Darlow, Stanisław Jastrzębski, and Amos Storkey. Latent adversarial debiasing: Mitigating collider bias in deep neural networks. *arXiv preprint arXiv:2011.11486*, 2020.
- [8] Sarah Jane Delany, Nicola Segata, and Brian Mac Namee. Profiling instances in noise reduction. *Knowledge-Based Systems*, 31:28–40, 2012.
- [9] Dragan Gamberger, Nada Lavrac, and Saso Dzeroski. Noise detection and elimination in data preprocessing: experiments in medical domains. *Applied artificial intelligence*, 14(2):205–223, 2000.
- [10] Robert Geirhos, Patricia Rubisch, Claudio Michaelis, Matthias Bethge, Felix A. Wichmann, and Wieland Brendel. Imagenet-trained CNNs are biased towards texture; increasing shape bias improves accuracy and robustness. In *International Conference on Learning Representations*, 2019.
- [11] Kaiming He, Xiangyu Zhang, Shaoqing Ren, and Jian Sun. Deep residual learning for image recognition. *arXiv preprint arXiv:1512.03385*, 2015.
- [12] Lisa Anne Hendricks, Kaylee Burns, Kate Saenko, Trevor Darrell, and Anna Rohrbach. Women also snowboard: Overcoming bias in captioning models. In *Proceedings of the European Conference on Computer Vision (ECCV)*, pages 771–787, 2018.
- [13] Zeyi Huang, Haohan Wang, Eric P. Xing, and Dong Huang. Self-challenging improves cross-domain generalization. In *ECCV*, 2020.
- [14] Lu Jiang, Zhengyuan Zhou, Thomas Leung, Li-Jia Li, and Li Fei-Fei. MentorNet: Learning data-driven curriculum for very deep neural networks on corrupted labels. In *Proceedings of the 35th International Conference on Machine Learning*, Proceedings of Machine Learning Research, 2018.
- [15] Byungju Kim, Hyunwoo Kim, Kyungsu Kim, Sungjin Kim, and Junmo Kim. Learning not to learn: Training deep neural networks with biased data. In *The IEEE Conference on Computer Vision and Pattern Recognition (CVPR)*, June 2019.
- [16] Eungyeup Kim, Jihyeon Lee, and Jaegul Choo. Biaswap: Removing dataset bias with bias-tailored swapping augmentation. In *Proceedings of the IEEE/CVF International Conference on Computer Vision (ICCV)*, pages 14992–15001, October 2021.
- [17] Yann LeCun and Corinna Cortes. MNIST handwritten digit database. 2010.
- [18] Jungsoo Lee, Eungyeup Kim, Juyoung Lee, Jihyeon Lee, and Jaegul Choo. Learning debiased representation via disentangled feature augmentation. In *Advances in Neural Information Processing Systems*, 2021.

- [19] Yi Li and Nuno Vasconcelos. Repair: Removing representation bias by dataset resampling. In *Proceedings of the IEEE Conference on Computer Vision and Pattern Recognition*, pages 9572–9581, 2019.
- [20] Junhyun Nam, Hyuntak Cha, Sungsoo Ahn, Jaeho Lee, and Jinwoo Shin. Learning from failure: Training debiased classifier from biased classifier. In *Advances in Neural Information Processing Systems*, 2020.
- [21] Shiori Sagawa, Pang Wei Koh, Tatsunori B Hashimoto, and Percy Liang. Distributionally robust neural networks for group shifts: On the importance of regularization for worst-case generalization. *arXiv preprint arXiv:1911.08731*, 2019.
- [22] Ramprasaath R. Selvaraju, Michael Cogswell, Abhishek Das, Ramakrishna Vedantam, Devi Parikh, and Dhruv Batra. Grad-cam: Visual explanations from deep networks via gradient-based localization. In *ICCV*, 2017.
- [23] Borut Sluban, Dragan Gamberger, and Nada Lavrač. Ensemble-based noise detection: noise ranking and visual performance evaluation. *Data mining and knowledge discovery*, 28(2):265–303, 2014.
- [24] Enzo Tartaglione, Carlo Alberto Barbano, and Marco Grangetto. End: Entangling and disentangling deep representations for bias correction. In *Proceedings of the IEEE/CVF Conference on Computer Vision and Pattern Recognition (CVPR)*, pages 13508–13517, June 2021.
- [25] A. Torralba and A. A. Efros. Unbiased look at dataset bias. *CVPR ’11*, 2011.
- [26] Haohan Wang, Zexue He, Zachary L. Lipton, and Eric P. Xing. Learning robust representations by projecting superficial statistics out. In *International Conference on Learning Representations*, 2019.
- [27] Tianlu Wang, Jieyu Zhao, Mark Yatskar, Kai-Wei Chang, and Vicente Ordonez. Balanced datasets are not enough: Estimating and mitigating gender bias in deep image representations. In *Proceedings of the IEEE/CVF International Conference on Computer Vision*, pages 5310–5319, 2019.
- [28] Virginia Whewey. Using boosting to detect noisy data. In *Pacific Rim International Conference on Artificial Intelligence*, pages 123–130. Springer, 2000.
- [29] Xiaobo Xia, Tongliang Liu, Bo Han, Mingming Gong, Jun Yu, Gang Niu, and Masashi Sugiyama. Sample selection with uncertainty of losses for learning with noisy labels. In *International Conference on Learning Representations*, 2022.
- [30] Zhilu Zhang and Mert R Sabuncu. Generalized cross entropy loss for training deep neural networks with noisy labels. *arXiv preprint arXiv:1805.07836*, 2018.

This supplementary presents the following: A) GradCAM [22] visualization of multiple f_B^* capturing diverse visual attributes, B) how BE further amplifies bias when training f_B , C) stable performance of using multiple BCDs, D) the comparisons of debiasing performance on the unbiased test sets with the standard deviation, E) the pseudo-code of our training procedure, F) performance degradation of BE with strict agreement votes, G) detailed descriptions of datasets, H) further implementation details, and I) the broader impacts and the limitation of our work.

A Visualization of Multiple f_B^* Capturing Diverse Visual Attributes

As mentioned in Section 4.2 of the main paper, we visualize how each f_B^* captures the bias attribute by using GradCAM [22] in Fig. 5 in order to demonstrate that biased models f_B^* with different random initialization focus on different visual attributes. For the visualization, we use BFFHQ of which the intrinsic attribute and the bias attribute are the age and the gender, respectively. We show images which all five f_B^* predict with the correct bias labels in Fig. 5. The first column indicates the original images while the other columns indicate the GradCAM of each f_B^* , respectively. We observe that each f_B^* focuses on different visual attributes. For example, $f_{B_1}^*$ focuses on the mouth for predicting the gender (*e.g.*, focusing on lip makeups for females and mustaches for males). On the other hand, $f_{B_3}^*$ and $f_{B_4}^*$ heavily rely on the hair for predicting the gender. Meanwhile, $f_{B_2}^*$ and $f_{B_5}^*$ uses the nose and eyes for making predictions.

As mentioned in the main paper, a bias (*e.g.*, gender) can be formed in a combination of multiple visual attributes (*e.g.*, hair, mustache, eyes, makeup, etc). However, in Fig. 5, we observe that each biased model only uses a certain visual cue (*e.g.*, mustache or hair) for making predictions, partially capturing the bias attribute. Utilizing multiple BCDs in our method mitigates such an issue since it regards an image as a bias-aligned one only if the image includes at least half number of visual attributes contributing the model to be biased. Such visualization demonstrates the necessity of ensembling multiple biased models compared to using a single one.

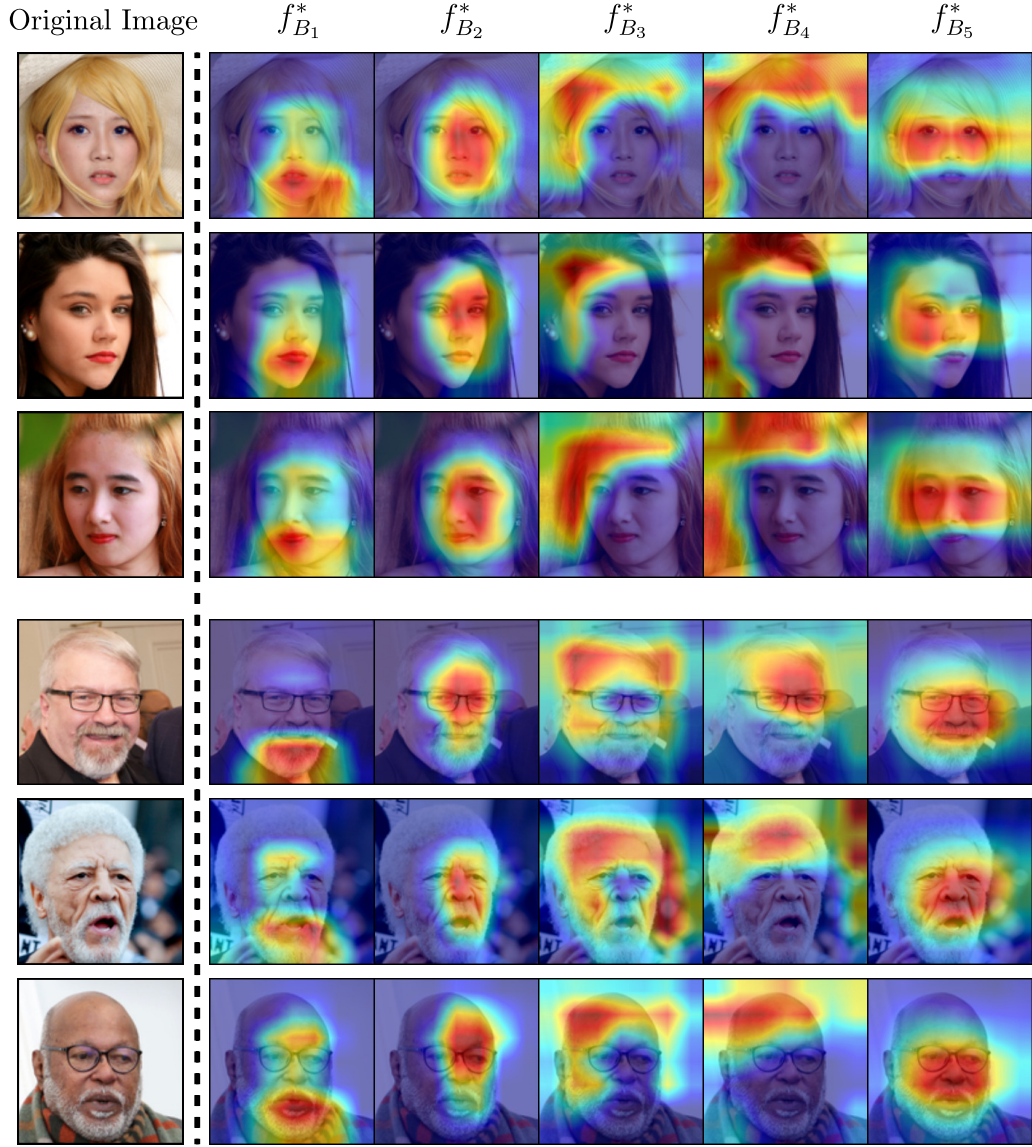


Figure 5: GradCAM of individual f_B^* . The first column indicates the original images. Starting from the second column, we visualize GradCAM using each biased model (*i.e.*, $f_{B_1}^*, \dots, f_{B_5}^*$).

B Amplified Bias via BE

Table 6 shows the image classification accuracy of f_B on the biased and unbiased test set. We compare LfF [20] without BE and LfF with BE using the test set accuracy at the last epoch in Table 6. As mentioned in the main paper, a biased model achieves 1) low accuracy on the unbiased test set and 2) high accuracy on the biased test set. In other words, the difference between the accuracy of the biased test set and that of the unbiased test set, acc_{diff} in Table 6, is high for the biased models. This is due to the fact that the biased model heavily relies on the bias attributes while failing to learn the intrinsic attributes.

As shown in Table 6, using BE significantly increases the acc_{diff} indicating that utilizing BE further amplifies bias for f_B . To be more specific, leveraging BE achieves low unbiased test set accuracy and high biased test set accuracy in Colored MNIST. Meanwhile, we observe a minimal performance drop in the biased test set with other datasets. However, considering the significant performance drop on the unbiased test set and high acc_{diff} , such a drop in biased test set accuracy is negligible. Such a result shows that the debiasing performance gain of BE is due to the amplified bias of f_B . It again demonstrates the fact that two factors are crucial for amplifying bias: 1) improving the biased test set accuracy of f_B and 2) degrading the unbiased test set accuracy of f_B (*i.e.*, not learning intrinsic attributes).

Table 6: Comparisons of f_B on the unbiased test set and the biased test set. Adding BE encourages f_B to be further biased in LfF. We use 1% ratio of bias-conflicting samples for each dataset. Applying BE on LfF is shaded in grey. For acc_{diff} , we compute the difference between the average of biased test set accuracy and that of unbiased test set accuracy.

Method	Colored MNIST			BFFHQ			Dogs & Cats			BAR		
	unbiased \downarrow	biased \uparrow	$\text{acc}_{\text{diff}}\uparrow$	unbiased \downarrow	biased \uparrow	$\text{acc}_{\text{diff}}\uparrow$	unbiased \downarrow	biased \uparrow	$\text{acc}_{\text{diff}}\uparrow$	unbiased \downarrow	biased \uparrow	$\text{acc}_{\text{diff}}\uparrow$
f_B of LfF [20]	15.02 ± 1.22	88.38 ± 14.61	73.36	55.84 ± 1.80	99.50 ± 0.21	43.66	36.3 ± 3.49	96.18 ± 0.62	59.88	69.07 ± 0.87	98.33 ± 0.78	29.26
f_B of LfF+BE	13.29 ± 1.61	99.10 ± 0.05	85.81	37.96 ± 1.77	98.9 ± 0.16	60.94	13.42 ± 1.42	94.35 ± 0.19	80.93	53.53 ± 2.90	96.00 ± 0.73	42.47

C Performance Variation of Single/Multiple BCDs

As mentioned in Section 5.3 of the main paper, utilizing multiple BCDs reduces the performance variations compared to using a single BCD. Fig. 6 demonstrates the fact by visualizing the metrics used in Fig. 1 of the main paper using Dogs & Cats dataset. The shaded regions indicate the performance variation, the differences of five independent trials on a given metric. We observe that utilizing multiple BCDs (red) shows smaller variations in terms of $w(x)$ of bias-conflicting samples and the unbiased test set accuracy of f_D . Again, this is due to the fact that leveraging multiple numbers of f_B^* enables to consider multiple visual attributes, better capturing and understanding the bias attribute compared to using a single f_B^* .

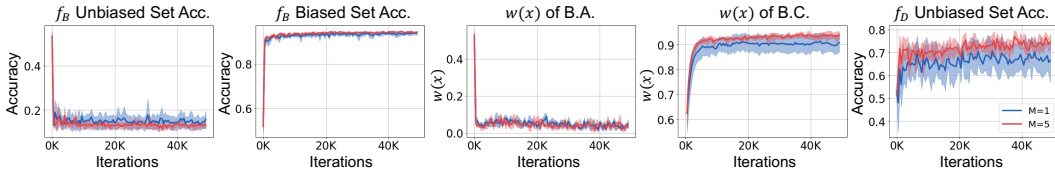


Figure 6: Comparison of models trained with 1) a single BCD ($M = 1$, blue) and 2) multiple BCDs ($M = 5$, red) on Dogs & Cats. The shaded areas show the variations of the results on five different independent trials. Each metric corresponds to the ones used in Fig. 1 of the main paper.

D Comparisons of Debiasing Performance on Unbiased Test Sets

Table 7: Image classification accuracies on unbiased test sets of Colored MNIST and Dogs & Cats with varying ratios of bias-conflicting samples. The *cross* and *check* represent whether each model 1) uses bias labels during training and 2) requires predefined bias type. For LfF and DisEnt, the performance gains are shaded in grey. Best performing results are marked in bold.

Method		Colored MNIST				Dogs & Cats	
		0.5%	1.0%	2.0%	5.0%	1.0%	5.0%
Vanilla [11]	XX	34.75 \pm 1.68	51.14 \pm 3.12	65.72 \pm 3.74	82.82 \pm 0.63	48.06 \pm 7.09	69.88 \pm 1.73
HEX [26]	X✓	42.25 \pm 1.83	47.02 \pm 15.08	72.82 \pm 1.03	85.50 \pm 1.94	46.76 \pm 5.3	72.60 \pm 3.01
LNL [15]	✓✓	36.29 \pm 0.77	49.48 \pm 5.29	63.30 \pm 2.73	81.30 \pm 0.80	50.90 \pm 4.62	73.96 \pm 1.86
EnD [24]	✓✓	35.33 \pm 1.23	48.97 \pm 11.54	67.01 \pm 2.81	82.09 \pm 2.20	48.56 \pm 5.69	68.24 \pm 2.24
ReBias [3]	X✓	60.86 \pm 1.96	82.78 \pm 1.36	92.00 \pm 0.47	96.45 \pm 0.17	48.70 \pm 6.05	65.74 \pm 0.51
LfF [20]	XX	63.55 \pm 6.97	76.81 \pm 4.56	84.18 \pm 1.15	89.65 \pm 0.49	71.72 \pm 4.56	84.32 \pm 1.87
DisEnt [18]	XX	68.49 \pm 3.36	79.99 \pm 2.15	84.09 \pm 1.46	89.91 \pm 0.55	65.74 \pm 3.31	81.58 \pm 2.44
LfF + BE		69.70 \pm 4.10	81.17 \pm 0.68	85.20 \pm 0.85	90.04 \pm 0.18	81.52 \pm 1.13	88.60 \pm 1.79
		(+ 6.15)	(+ 4.36)	(+ 1.02)	(+ 0.39)	(+ 9.80)	(+ 4.28)
DisEnt + BE		71.34 \pm 1.30	82.11 \pm 0.54	84.66 \pm 1.72	90.15 \pm 0.48	80.74 \pm 2.80	86.84 \pm 0.77
		(+ 2.85)	(+ 2.12)	(+ 0.57)	(+ 0.24)	(+ 15.00)	(+ 5.26)

Table 8: Image classification accuracies on unbiased test sets of BFFHQ and BAR with varying ratios of bias-conflicting samples. The *cross* and *check* represent whether each model 1) uses bias labels during training and 2) requires predefined bias type. For LfF and DisEnt, the performance gains are shaded in grey. Best performing results are marked in bold.

Method		BFFHQ				BAR	
		0.5%	1.0%	2.0%	5.0%	1.0%	5.0%
Vanilla [11]	XX	55.64 \pm 0.44	60.96 \pm 1.00	69.00 \pm 0.50	82.88 \pm 0.49	70.55 \pm 0.87	82.53 \pm 1.08
HEX [26]	X✓	56.96 \pm 0.62	62.32 \pm 1.21	70.72 \pm 0.89	83.40 \pm 0.34	70.48 \pm 1.74	81.20 \pm 0.68
LNL [15]	✓✓	56.88 \pm 1.13	62.64 \pm 0.99	69.80 \pm 1.03	83.08 \pm 0.93	70.65 \pm 1.28	82.43 \pm 1.25
EnD [24]	✓✓	55.96 \pm 0.91	60.88 \pm 1.17	69.72 \pm 1.14	82.88 \pm 0.74	71.07 \pm 2.03	82.78 \pm 0.30
ReBias [3]	X✓	55.76 \pm 1.50	60.68 \pm 1.24	69.60 \pm 1.33	82.64 \pm 0.64	73.04 \pm 1.04	83.90 \pm 0.82
LfF [20]	XX	65.19 \pm 3.23	69.24 \pm 2.07	73.08 \pm 2.70	79.80 \pm 1.09	70.16 \pm 0.77	82.95 \pm 0.27
DisEnt [18]	XX	62.08 \pm 3.89	66.00 \pm 1.33	69.92 \pm 2.72	80.68 \pm 0.25	70.33 \pm 0.19	83.13 \pm 0.46
LfF + BE		67.36 \pm 3.10	75.08 \pm 2.29	80.32 \pm 2.07	85.48 \pm 2.88	73.36 \pm 0.97	83.87 \pm 0.82
		(+ 2.17)	(+ 5.84)	(+ 7.24)	(+ 5.68)	(+ 3.20)	(+ 0.92)
DisEnt + BE		67.56 \pm 2.11	73.48 \pm 2.12	79.48 \pm 1.80	84.84 \pm 2.11	73.29 \pm 0.41	84.96 \pm 0.69
		(+ 5.48)	(+ 7.48)	(+ 9.56)	(+ 4.16)	(+ 2.96)	(+ 1.83)

Due to the page limit, we intentionally omitted the standard deviation in Table 1 of the main paper. Therefore, we present the quantitative results on the unbiased test sets including the standard deviations in Table 7 and Table 8. Note that the results are averaged over five individual trials.

E Pseudo-code of Our Training Procedure

For a better understanding of our proposed method, we describe the training procedure of utilizing BE on existing reweighting-based debiasing methods using a pseudo-code.

Algorithm 1 BE added to reweighting-based debiasing methods

Input: iteration for pretraining t_B , dataset \mathcal{D} , confidence threshold τ , the number of biased models used in BE M

Initialize biased models $f_{B_1}^*, \dots, f_{B_M}^*$ ▷ Pretrain biased models

for $t = 1, 2, \dots, t_B$ **do**
 | Update $f_{B_1}^*, \dots, f_{B_M}^*$ using \mathcal{D} with \mathcal{L}_{GCE}

end

$\mathcal{D}_A \leftarrow \emptyset$ ▷ Construct the bias-amplified dataset \mathcal{D}_A

for $(x, y) \in \mathcal{D}$ **do**
 for $f \in \{f_{B_1}^*, \dots, f_{B_M}^*\}$ **do**
 if $p_y(x; f) < \tau$ **then**
 | $BCD(x; \tau, f) \leftarrow 0$
 else
 | $BCD(x; \tau, f) \leftarrow 1$
 end
 end
 if $\sum_{i=1}^M BCD(x; \tau, f_{B_i}^*) \geq \lceil \frac{M}{2} \rceil$ **then**
 | $\mathcal{D}_A \leftarrow \mathcal{D}_A \cup \{(x, y)\}$
 end

end

Initialize two networks f_B, f_D ▷ Train a debiasing model

while *not converged* **do**
 for $(x, y) \in \mathcal{D}$ **do**
 Compute reweighting value $w(x)$ using f_B and f_D
 if $(x, y) \in \mathcal{D}_A$ **then**
 | Update f_B using \mathcal{D}_A with $\mathcal{L}_{\text{CE}}(f_B(x), y)$
 end
 Update f_D using \mathcal{D} with $w(x) \cdot \mathcal{L}_{\text{CE}}(f_D(x), y)$
 end

end

F BE with Strict Agreements

As mentioned in Section 5.3 of the main paper, two factors are crucial for constructing a bias-amplified dataset \mathcal{D}_A : 1) discarding a sufficient number of bias-conflicting samples and 2) maintaining a reasonable number of bias-aligned ones. We further demonstrate such a point by designing a strict version of BE in Table 9; we regard a sample as a bias-conflicting one only if all five BCDs consider it as a bias-conflicting sample. \mathcal{N}_a in Table 9 indicates the number of agreement votes required for deciding a sample as a bias-conflicting one. We add BE on LfF [20] with \mathcal{N}_a set to three and five, and compare them with the original LfF. Note that the number of BCDs, M , is fixed to five.

Utilizing BE with $\mathcal{N}_a=5$ outperforms the original LfF. However, we observe that utilizing BE with $\mathcal{N}_a=3$ is superior to BE with $\mathcal{N}_a=5$. The main reason is due to the number of bias-aligned and bias-conflicting samples. Similar to Table 4 of the main paper, we report the remaining samples of bias-aligned samples and bias-conflicting samples in \mathcal{D}_A by showing the adjusted ratio compared to each group in \mathcal{D} . We observe that utilizing BE with $\mathcal{N}_a=5$ discards the bias-conflicting ones significantly while also filtering out a considerable number of the bias-aligned ones. For example, by utilizing $\mathcal{N}_a=5$ in BFFHQ, there exist only 2.29% of bias-conflicting samples in \mathcal{D}_A compared to \mathcal{D} . However, only 57.48% of bias-aligned samples are remained in \mathcal{D}_A , limiting f_B to be further biased.

Table 9: Unbiased test set accuracies and remaining samples in \mathcal{D}_A depending on the number of agreement votes for discarding bias-conflicting samples. Using $\mathcal{N}_a=5$ rather aggravates the debiasing performance since it discards a significant number of bias-aligned samples which is important for constructing a bias-amplified dataset \mathcal{D}_A .

Dataset	Unbiased test set accuracy			Remaining samples in \mathcal{D}_A			
	LfF	$\mathcal{N}_a=5$	$\mathcal{N}_a=3$	# of B.A.(%) \uparrow		# of B.C.(%) \downarrow	
				$\mathcal{N}_a = 5$	$\mathcal{N}_a = 3$	$\mathcal{N}_a = 5$	$\mathcal{N}_a = 3$
Colored MNIST	76.81 \pm 4.56	80.51 \pm 0.88	81.17 \pm 0.68	96.80 \pm 1.06	99.96 \pm 0.03	0.00 \pm 0.00	1.42 \pm 0.78
BFFHQ	69.24 \pm 2.07	70.00 \pm 1.44	75.08 \pm 2.29	57.48 \pm 7.36	92.22 \pm 0.26	2.29 \pm 1.08	24.37 \pm 3.07
Dogs & Cats	71.72 \pm 4.56	76.86 \pm 2.11	81.52 \pm 1.13	57.84 \pm 1.52	88.60 \pm 1.02	1.00 \pm 0.56	9.50 \pm 3.75
BAR	70.16 \pm 0.77	71.84 \pm 1.22	73.36 \pm 0.97	63.79 \pm 0.81	98.39 \pm 0.19	5.71 \pm 3.19	51.42 \pm 5.34

G Further Details on Datasets

Colored MNIST. We modify MNIST dataset [17] and set the color as the bias attribute. Each one of the ten digits is highly correlated with a certain color (*e.g.*, red for 0). We inject the color into the foreground of each image. For Colored MNIST, we conduct experiments with the dataset used in Lee *et al.* [18]. For each ratio of bias-conflicting samples, the number of bias-aligned samples and bias-conflicting samples are as follows: (54751, 249)-0.5%, (54509, 491)-1%, (54014, 986)-2%, and (52551, 2449)-5%.

BFFHQ. We used BFFHQ which was first introduced in Kim *et al.* [16]. BFFHQ set the age (*i.e.*, old and young) as the intrinsic attribute and the gender as the bias attribute. Bias-aligned samples are young (*i.e.*, age ranging from 10 to 29) females and old (*i.e.*, age ranging from 40 to 59) males. For each ratio of bias-conflicting sample, the number of bias-aligned samples and bias-conflicting samples are as follows: (19104, 96)-0.5%, (19008, 192)-1%, (18816, 384)-2%, and (18240, 960)-5%. Following the work of Lee *et al.*, we exclude the bias-aligned samples from the unbiased test set since it only includes two target classes [18].

Dogs & Cats. Dogs & Cats [1] was first used in Kim *et al.* [15]. However, we find that the test sets used in the work do not have publicly available ground truths. Therefore, since the original train set has ground truth labels, we split the original train set into train, valid, and test sets. For each ratio of bias-conflicting sample, the number of bias-aligned samples and bias-conflicting samples are as follows: (8037, 80)-1% and (8037, 452)-5%. We did not include the bias-aligned samples in the unbiased test set.

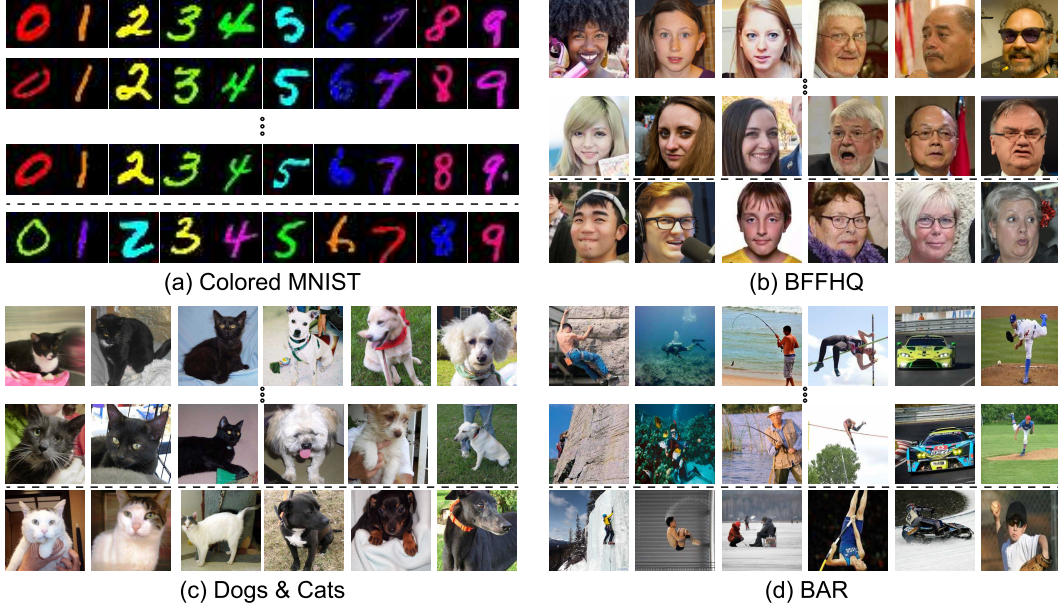


Figure 7: Illustrative example of the datasets used in our work. For better understanding, we present a bigger figure of datasets compared to the one in the main paper.

BAR. In the work of Nam *et al.*, the original BAR dataset does not include bias-conflicting samples in the training set. However, for the consistent experimental setting and for the evaluation under various bias severities, we build two sets of BAR dataset with different ratios of bias-conflicting samples. For each ratio of bias-conflicting sample, the number of bias-aligned samples and bias-conflicting samples are as follows: (1761, 14)-1% and (1761, 85)-5%. We did not include the bias-aligned samples in the unbiased test set.

H Further Implementation Details

Experimental settings. We set the learning rate as 0.01, 0.0001, 0.0001, and 0.00001 for Colored MNIST, BFFHQ, Dogs & Cats, and BAR, respectively. The image sizes are 28×28 for Colored MNIST and 224×224 for the rest of the datasets. For Colored MNIST, we do not apply additional data augmentation techniques. For BFFHQ, Dogs & Cats, and BAR, we apply random crop and horizontal flip transformations. Also, images are normalized along each channel (3, H, W) with the mean of (0.4914, 0.4822, 0.4465) and standard deviation of (0.2023, 0.1994, 0.2010). We conducted all experiments using a single V100 GPU. Reweighting-based debiasing methods (*e.g.*, LfF [20] and DisEnt [18]) requires approximately up to 6GB of memory.

Applying BE on Reweighting-based Methods. As aforementioned in Section 4.3 of the main paper, when applying BE to existing reweighting-based approaches (*i.e.*, LfF [20] and DisEnt [18]), we do not modify the training procedure of the debiased model f_D . For both methods, we train f_B using the bias-amplified dataset \mathcal{D}_A . DisEnt, unlike LfF, additionally utilizes feature-level data augmentation during training. When we apply BE to DisEnt, we use \mathcal{D}_A for training the parameters which are updated with respect to the feature vectors of bias attributes. f_B of our paper corresponds to E_b and C_b in the original paper of DisEnt [18].

I Discussion

Social/Broader Impacts As we are living in the era of deep learning, we have recently witnessed numerous well-working deep learning models in various fields. Deep learning models generally rely on the training set, so the way training set is designed may decide the predictions of the deep learning

models. In this perspective, a model trained with a biased dataset without additional supervision may have no chance to make unbiased decisions. This could be problematic when deep learning models are on deployment. For example, if a deep learning based recruitment system is biased towards the gender, a certain group of gender may be discriminated due to the gender bias. Our paper tries to mitigate such an important social issue and inspire future researchers by emphasizing the overlooked component of debiasing, f_B , to solve it.

Limitation One limitation of our work is that there still exist a small number of bias-conflicting samples in \mathcal{D}_A after applying BE. Ideally, a model trained with bias-aligned samples only would be perfectly biased towards the bias attribute. Since we do not use explicit bias labels, we could not discard all bias-conflicting samples when constructing \mathcal{D}_A for training f_B . In the meanwhile, we filtered out a sufficient amount of bias-conflicting samples, improving the debiasing performance of f_D which has been demonstrated throughout the paper.